Electronic Supplementary Material (ESI) for Journal of Materials Chemistry A.

Supplementary Information

Synthesis of graphene mesosponge via catalytic methane decomposition on magnesium oxide

Shogo Sunahiro,[a] Keita Nomura,[b] Shunsuke Goto,[b] Kazuya Kanamaru,[b] Rui Tang,[c] Masanori Yamamoto,[b] Takeharu Yoshii,[b] Junko N. Kondo,[d] Qi Zhao,[e] Azeem Ghulam Nabi,[e] Rachel Crespo-Otero,[e] Devis Di Tommaso,[e] Takashi Kyotani[b] and Hirotomo Nishihara[bc]*

[a]R & D Strategy Division, Tokai Carbon Co., Ltd., Aoyama Building, 1-2-3 Kita Aoyama, Minato-ku, Tokyo, 107-8636, Japan

[b]Institute of Multidisciplinary Research for Advance Materials, Tohoku University, 2-1-1 Katahira, Aoba-ku, Sendai, Miyagi, 980-8577, Japan.

[c]Advanced Institute for Materials Research, Tohoku University, 2-1-1 Katahira, Aoba-ku, Sendai, Miyagi, 980-8577, Japan.

[d]Institute of Innovative Research, Tokyo Institute of Technology, 4259 Nagatsuda Midori-ku, Yokohama 226-8503, Japan

[e]School of Biological and Chemical Sciences, Queen Mary University of London, Mile End Road, London E1 4NS, United Kingdom

**E-mail: hirotomo.nishihara.b1@tohoku.ac.jp*

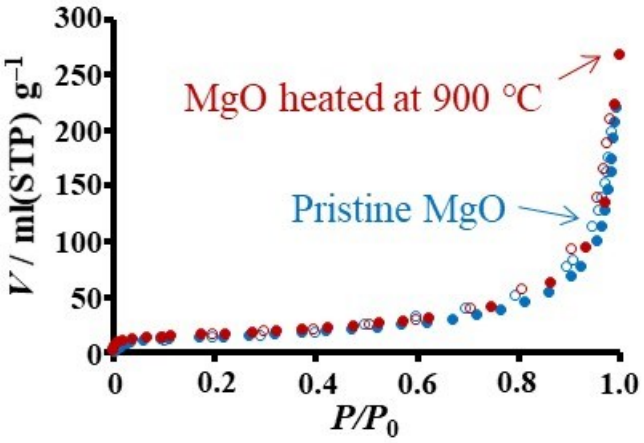

Fig. S1 N_2 adsorption/desorption isotherms of MgO before and after the heat treatment at 900 °C. The amount of N_2 adsorption of MgO after the heat treatment slightly increases at a low P/P_0, and the specific surface area is increased from 50 to 61 m^2 g^{-1} by the heat treatment.

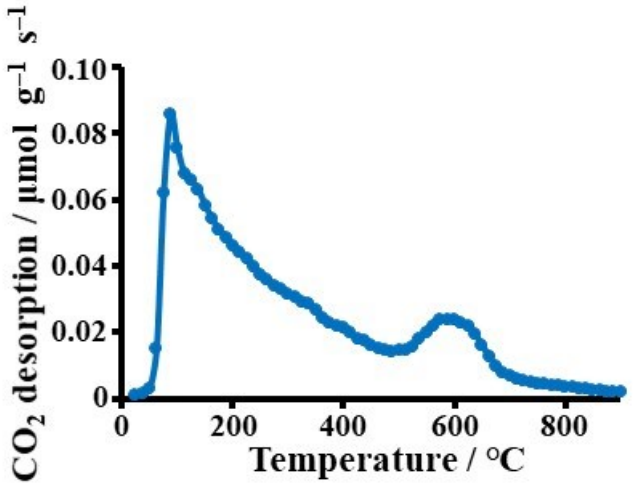

Fig. S2 The profiles of CO_2-TPD on MgO pre-heated at 500 °C.

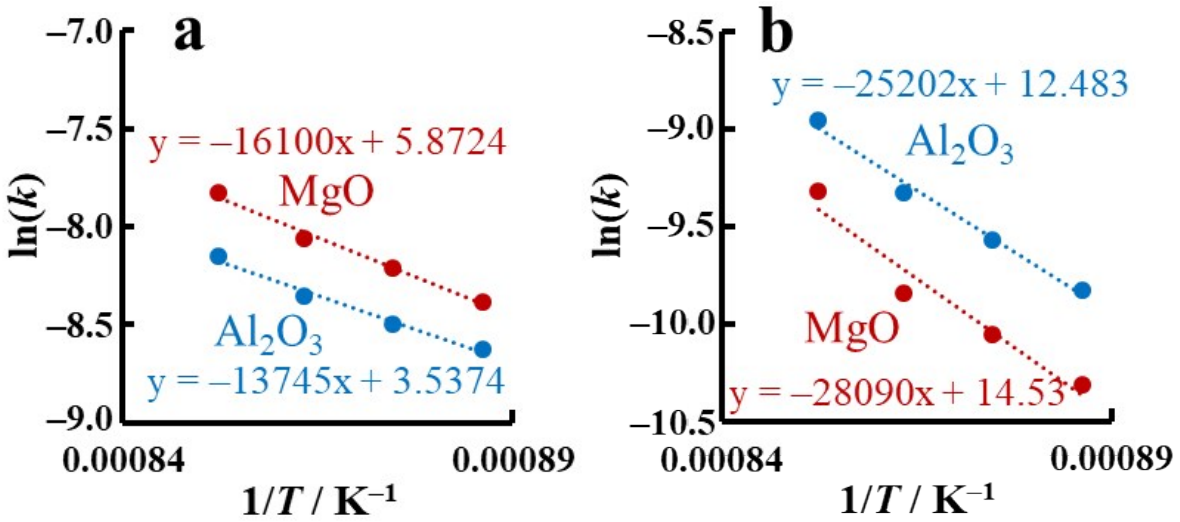

Fig. S3 The Arrhenius plots of catalytic methane decomposition on MgO and Al_2O_3 at (a) $N_{stack} < 1$ and (b) $N_{stack} > 1$.

Table S1 Calculated reaction enthalpy (H_f) and activation energies for the forward ($E_{a,f}^+$) and reverse ($E_{a,r}^+$) elementary steps involved in the C–H activation on MgO(100) surface. Values in eV.

	Forward activation energy	**Enthalpy**	**Reverse activation energy**
Reaction	**$E_{a,f}^+$**	**H_f^+**	**$E_{a,r}^+$**
$CH_4 \rightarrow CH_3 + H$	4.55	2.51	2.04
$CH_3 \rightarrow CH_2 + H$	4.27	1.46	2.81
$CH_2 \rightarrow CH + H$	4.14	3.01	1.13
$CH \rightarrow C + H$	3.85	2.26	1.59

Table S2 Calculated reaction enthalpy (H_f) and activation energies for the forward ($E_{a,f}^+$) and reverse ($E_{a,r}^+$) elementary steps involved in the C–H activation on Mg(110) surface. Values in eV.

	Forward activation energy	**Enthalpy**	**Reverse activation energy**
Reaction	**$E_{a,f}^+$**	**H_f^+**	**$E_{a,r}^+$**
$CH_4 \rightarrow CH_3+H$	0.84	-0.36	1.20
$CH_3 \rightarrow CH_2+H$	2.54	0.40	2.14
$CH_2 \rightarrow CH+H$	2.98	1.48	1.50
$CH \rightarrow C+H$	3.42	1.83	1.59

Table S3 Calculated reaction enthalpy (H_f) and activation energies for the forward ($E_{a,f}^+$) and reverse ($E_{a,r}^+$) elementary steps involved in the C–H activation on MgO(110) surface with a vacant O site. Values in eV.

	Forward activation energy	**Enthalpy**	**Reverse activation energy**
Reaction	**$E_{a,f}^+$**	**H_f^+**	**$E_{a,r}^+$**
$CH_4 \rightarrow CH_3+H$	0.65	0.3	0.35
$CH_3 \rightarrow CH_2+H$	2.73	1.33	1.40
$CH_2 \rightarrow CH+H$	1.39	-0.3	1.69
$CH \rightarrow C+H$	3.12	0.6	2.52

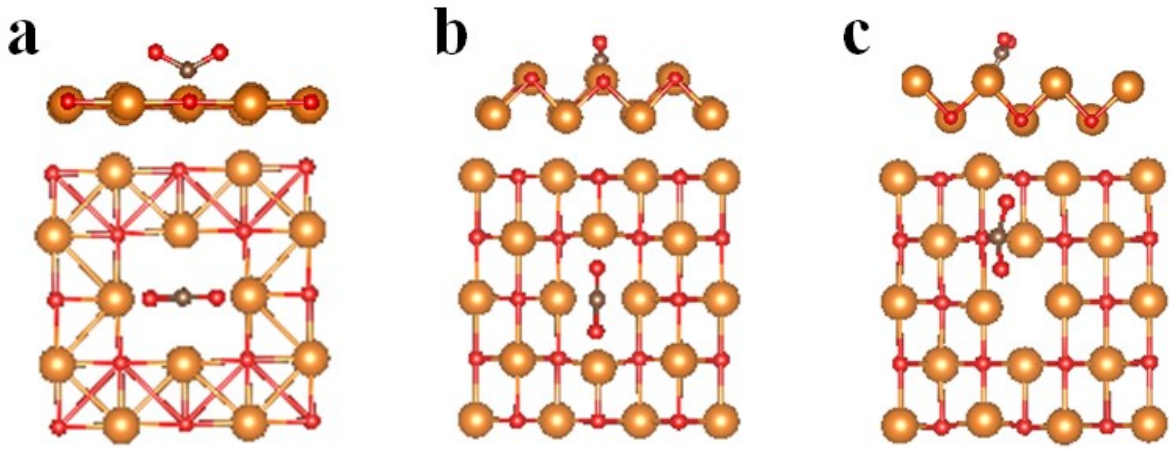

Fig. S4 Illustrations for the calculation of CO_2 adsorption on MgO surface structures. (a) Flat MgO(100) surface with a vacant O site, MgO(100)V_O. (b) Stepped MgO(110) surface with a vacant top-site O, MgO(110)V_O-top. (c) Stepped MgO(110) surface with a bottom-site O, MgO(110)V_O-bottom.

Table S4 Calculated adsorption energies of CO_2 on the flat MgO(100) surface with a vacant O site, MgO(100) V_O, and on the stepped MgO(110) surface with a vacant top-site O, V_O-top, and bottom-site O, V_O-bottom. Values in eV.

	Adsorption energy
MgO(100)Vo	-0.91
MgO(110)Vo-top	-3.39
MgO(110)Vo-bottom	-1.10

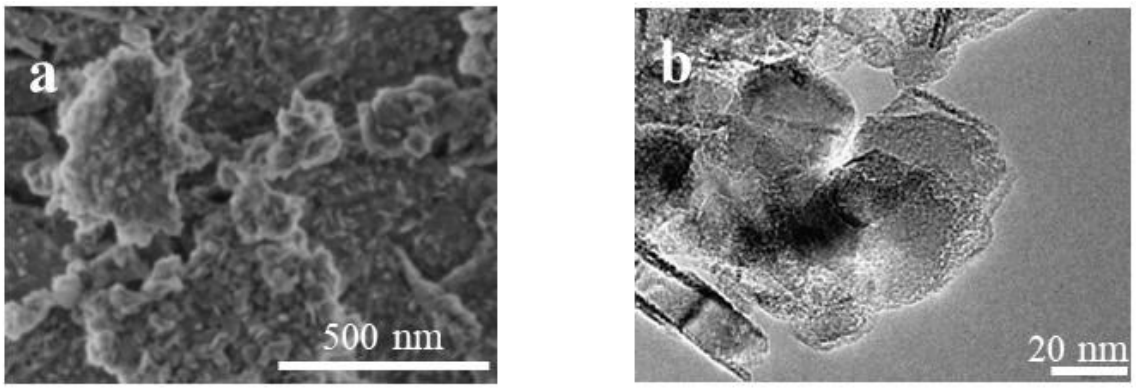

Fig. S5 (a) SEM image of the pristine MgO. (b) TEM image of the pristine MgO.

Table S5 Gas emission amount of CO, CO_2, H_2O, and H_2 during high-sensitivity vacuum TPD and elemental compositions of O and H.

Sample	N_{CO} [a] (mmol g^{-1})	N_{CO2} [b] (mmol g^{-1})	N_{H2O} [c] (mmol g^{-1})	N_{H2} [d] (mmol g^{-1})	$N_{CO} + N_{H2}$ (mmol g^{-1})	O [e] (wt%)	H [f] (wt%)
YP-50F	0.98	0.07	0.26	2.12	3.10	2.21	0.48
XC72	0.19	0.03	0.07	0.41	0.60	0.51	0.10
KB	0.17	0.02	0.05	0.98	1.15	0.42	0.21
BP	0.28	0.12	0.07	0.61	0.89	0.94	0.14
DB	1.6	0.08	0.21	0.45	2.05	3.15	0.13
CMS(Al_2O_3)	0.85	0.13	0.28	1.06	1.91	2.21	0.27
GMS(Al_2O_3)	0.07	0.01	0.03	0.04	0.11	0.21	0.01
CMS(MgO)	0.95	0.13	0.34	0.91	1.86	2.48	0.25
GMS(MgO)	0.02	0.01	0.03	0.02	0.05	0.10	0.01

[a] CO emission amount.
[b] CO_2 emission amount
[c] H_2O emission amount.
[d] H_2 emission amount.
[e] O content calculated from the gas emission amount of CO, CO_2, and H_2O.
[f] H content calculated from the gas emission amount of H_2O and H_2.

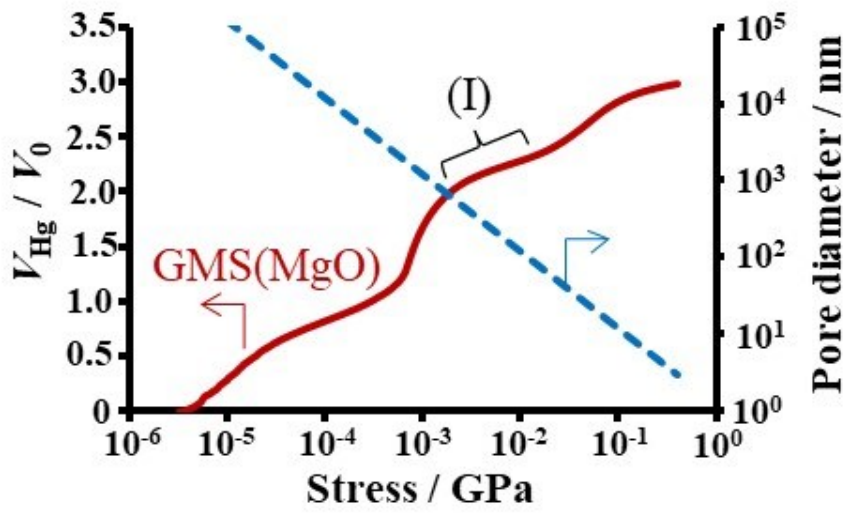

Fig. S6 V_{Hg}/V_0 versus stress loaded to MgO-derived GMS via Hg, which is measured by mercury porosimetry. The equation (8) gives the Hg pressure (P) at which the pores with the radius of r are impregnated by Hg, and the relation of $2r$ (pore diameter) and P is shown by a blue dashed line. The region (I) corresponds to stress-strain curve of GMS, and the bulk modulus can be calculated as 0.05 GPa.

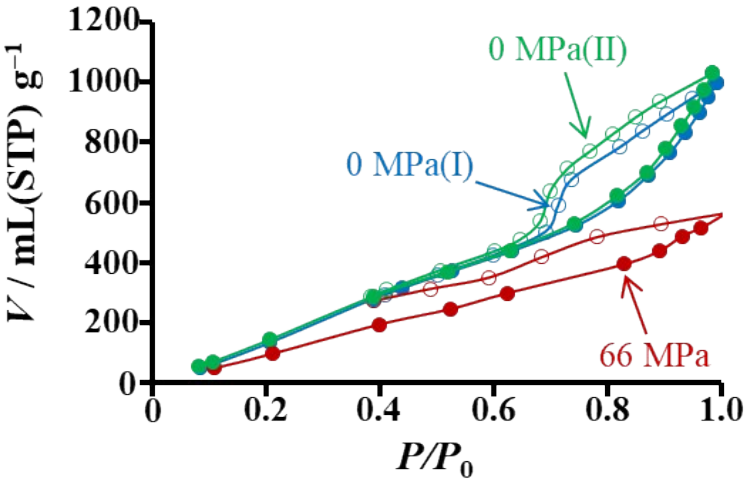

Fig. S7 Methanol adsorption-desorption isotherms of MgO-derived GMS at 25 °C with and without loading mechanical force: before loading force (0 MPa(I)), loading 66 MPa, and after recovered to 0 MPa (0 MPa(II)).